Synopsis of thesis entitled

"Anchored Silicotungstates: Synthesis, Characterization and Conversion of some Bioplatform molecules into Value added products"

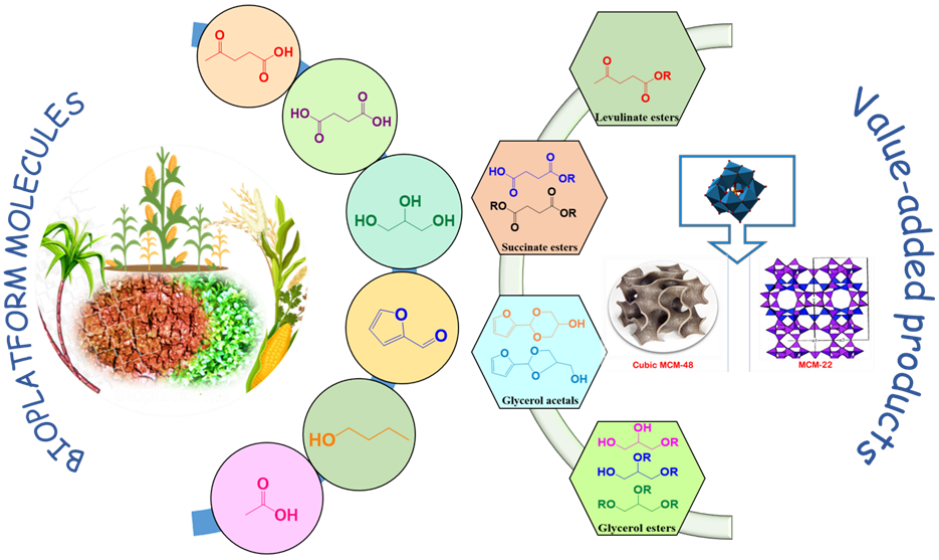

To be submitted to

The Maharaja Sayajirao University of Baroda

For the Degree of

DOCTOR OF PHILOSOPHY

IN

CHEMISTRY

By

Dhruvi Pithadia

Department of Chemistry
Faculty of Science
The Maharaja Sayajirao University of Baroda
Vadodara-390020, Gujarat, India

April, 2022

Introduction

In recent times, the upsurge in the demand of liquid fuel consumption and the diminishing fossil fuels to supply the global energy demand have attracted a worldwide mass of prospect scientists. This emerging research across the globe is driven by the rising shortage of fossil fuels, concerns regarding global warming and the increase in oil charges. Henceforth this challenging task can be addressed by replacing the non-renewable fossils by renewable biomass and inventing excellent sustainable technologies for production of biofuels biofuel additives and valuable chemicals from non-edible feedstock and judiciously selected bio-platforms, thus thereby building a base for future bio-based refineries[1].

The ultimate biorefinery concept is a germane research area, and these future findings hold their roots in an amazing capability of biomass, as an excellent alternative source to depleting non-renewable fossils. Nevertheless, the transformation of large biomass feedstock to simpler molecules is a challenging and developing domain. In this direction, valorization of platform chemicals, that are obtained from biomass can become a commencing objective for converting biobased feedstock to valuable chemicals, commodity materials and biofuels [2,3].

A biological material, biomass is a renewable energy source, derived from plants and animals or living organism. Future green and sustainable chemistry will rely on the creation of new product supply chains based on platform molecules derived from biomass. Although there is a large body of reported work on the production of these bioplatform molecules, it is very important to develop effective processes for adding value to these compounds through clean and efficient downstream chemistry. This can be achieved by catalysis which offers relevant possibility for sustainable production[4,5].

In the last two decades, the use of polyoxometalates (POMs) as catalysts has gained tremendous interest and open new expectations. By using polyoxometalates based catalysts, it is frequently possible to obtain higher selectivity and successfully solve ecological problems. They have several advantages as catalysts which make them economically and environmentally attractive. They have unique set of physicochemical properties that are of great value for catalysis. Among them the most important are well defined structure and strong Bronsted acidity. Their versatility and accessibility have led to many applications in various areas[6,7]. An additional attractive aspect

of POMs in catalysis is their inherent stability toward oxygen donors [8–10]. The acidic as well as redox properties of POMs are a function of the nature of the metal atoms (addenda atoms) and of both the heteroatom and the counter ions. The structural reorganization of POMs occurs in the solution state depending on the conditions such as temperature, concentrations, and pH of the solution[6].

The replacement of one or more addenda atoms is expected to tune the acidic as well as redox properties, which may lead to the development of active and selective catalysts. These are called as lacunary POMs (LPOM). Removal of one MO units from the fully occupied POM silicotungstic acid **$[SiW_{12}O_{40}]^{4-}$** (SiW_{12}**)**, giving rise to LPOM: mono lacunary **$[SiW_{11}O_{39}]^{8-}$** (SiW_{11}) (Figure 1).

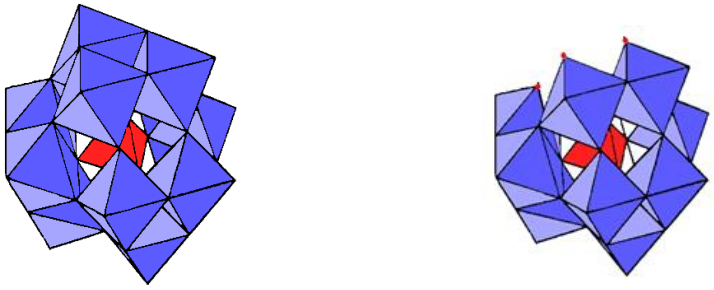

$[SiW_{12}O_{40}]^{4-}$ **$SiW_{11}O_{39}]^{8-}$**

Figure 1. Parent silicotungstic acid and Mono lacunary silicotungstate

Polyoxometalates are less corrosive and produce low amount of waste than conventional acid catalysts, they can be used as replacement in environmentally benign processes. As non-toxic crystalline substances, they are also preferable with regard to safety and ease of handling.

Keeping in mind these mentioned things; we have chosen silicotungstate based POMs for synthesis, characterization and catalytic applications because of some of its unique properties,

- Best amongst POMs in terms of hydrothermal stability
- Second best in terms of acidity after phosphotungstates
- Ease of synthesis
- Act as very good acid catalyst in homogeneous medium
- Still catalysis by Silicotungstates is less explored

Though, there are many advantages, the major disadvantages of polyoxometalates in homogeneous medium are solubility in polar medium, tedious separation of catalyst from reaction mixture and low thermal stability. The supporting of **POM** and **LPOM** on the suitable support is expected to overcome the above-mentioned problems. Synthesizing heterogeneous catalysis of POM and LPOM will be an attractive synthetic tool, particularly because it often satisfies some of the principles of green chemistry.

- It allows selectively to conduct different transformations by tuning some simple reactions parameters
- Easily accessible reaction conditions
- High thermal stability, increased surface area, high catalytic activity and selectivity
- Catalyst system can be conveniently recovered and recycled
- Product can be easily separated

Amongst various available supports, mesoporous and zeolitic supports are unique due to their interesting properties. MCM-48 and MCM-22 are of immense interest due to their unique pore networks, 3D cubic and 2D sinusoidal, respectively[11–14]. The pores are large enough to accommodate POMs in their channels. The loading of POMs on the mesoporous materials not only allows transfer of POMs catalyzed reactions from homogeneous to heterogeneous medium but also effectively increases the surface area of POMs. The perfect pore size of these materials benefits the easy access of reactants and products.

Keeping in mind the importance of conversion of Bioplatform molecules as well as development of new heterogeneous catalysts, it was thought to develop efficient heterogeneous catalysts comprising parent silicotungstic acid (SiW_{12}) as well as mono lacunary silicotungstate (SiW_{11}) and porous materials (MCM-48 and MCM-22), the objectives of this work are planned.

Objectives

- To synthesize and characterize a silica support, MCM-48
- To tune the acidic properties of parent silicotungstic acid (SiW_{12}) by designing at molecular level (formation of mono lacunary silicotungstate, (SiW_{11})
- To synthesize heterogeneous catalysts by anchoring SiW_{12} and SiW_{11} onto different supports (Synthesized MCM-48 and commercially acquired MCM-22)
- To characterize the synthesized catalysts by TGA, FT-IR, XRD, BET surface area and pore size distribution, SEM, TEM and acidic properties by n-butylamine and potentiometric titration
- To carry out the potential transformations of bioplatform molecules such as, Levulinic acid, Succinic acid, and Glycerol into value added products via Esterification and acetalization.
- To identify the activation energy and to study the mechanistic pathway of the proposed reactions
- To study the regeneration and recycling of the catalysts
- To study the effect of active species as well as the support on the catalytic activity
- To select the best catalyst based on the performance for the said reactions under similar reaction conditions

The work is divided into two parts

Part A: Silicotungstates anchored to MCM-48

Chapter 1: Parent Silicotungstic acid (SiW_{12}) anchored to MCM-48: Synthesis, characterization and esterification as well as acetalization reactions

Chapter 2: Mono lacunary Silicotungstate (SiW_{11}) anchored to MCM-48: Synthesis, characterization and esterification as well as acetalization reactions

Part B: Silicotungstates anchored to MCM-22

Chapter 1: Parent Silicotungstic acid (SiW_{12}) anchored to MCM-22: Synthesis, characterization and esterification as well as acetalization reactions

Chapter 2: Mono lacunary Silicotungstate (SiW_{11}) anchored to MCM-22: Synthesis, characterization and esterification as well as acetalization reactions

Annexure: Catalytic degradation of some organic dyes over SiW_{12} anchored nMCM-48 and MCM-22 catalysts

Part A

Chapter 1: Parent Silicotungstic acid (SiW_{12}) anchored to MCM-48: Synthesis, characterization and esterification as well as acetalization reactions

Synthesis of support MCM-48 and the catalysts

The synthesis of MCM-48 was carried out, by following the reported method with some modification[12]. To 50 g of distilled water, CTAB surfactant (2.4 g, 6.6 mmol) was added and allowed to dissolve completely at 35 ˚C. To this solution, ethanol (50 ml, 0.87 mmol) and 25 % wt liquor ammonia (~15.4 ml, 0.225 mol) was added and stirred for 15-20 mins, following dropwise addition of TEOS (3.4 g, 16 mmol). The resulting white suspension was aged for 2 h, filtered and washed with distilled water, dried at room temperature and calcined at 550 ˚C for 6 h. The material obtained was designated as nMCM-48.

A series of catalysts containing 10-40 % of TSA anchored to nMCM-48 were synthesized by wet impregnation method. 1 g of nMCM-48 was impregnated with an aqueous solution of TSA (0.1 g/ 10 mL – 0.4 g/ 40 mL of double distilled water) and dried at 100 ˚C for 10 h. The obtained catalysts were designated as TSA_1/nMCM-48, TSA_2/nMCM-48, TSA_3/nMCM-48, and TSA_4/nMCM-48, respectively.

Characterizations

The synthesized materials were characterized by potentiometric titrations (acidity measurement), BET surface area, elemental analysis, TGA, FT-IR, Powder XRD, ^{29}Si MAS NMR, SEM and TEM.

The acidic strength and total number of acidic sites of synthesized catalysts including support were determined by potentiometric titration. The acid strength of surface sites can be assigned according to the following scale: $Ei > 100$ mV (very strong sites), $0 < Ei < 100$ mV (strong sites), $-100 < Ei < 0$ mV (weak sites) and $Ei < -100$ mV (very weak sites)[15]. From the data presented in Table 1, it is well distinct that as the amount of SiW_{12} loading on nMCM-48 increases from 10 – 30 %, the acidic strength increases significantly, while negligible change observed from 30 – 40 %. The increase in number of very strong and strong acidic sites is directly related to the amount of SiW_{12} which is attributed to enhanced Bronsted acid sites.

Table 1. Acidity measurement and textural properties of nMCM-48 and catalysts

Material	Potentiometric titration				Textural Properties		
	Acidic strength (mV)	Types of acidic sites ($mEquig^{-1}$)		Total No. of acidic sites ($mEquig^{-1}$)	BET Surface area (m^2/g)	Pore diameter (Å)	Pore Volume (cm^3/g)
		Very strong	Strong				
nMCM-48	168	0.1	2.3	2.4	1307	20.8	0.63
$(SiW_{12})_1$/nMCM-48	646	0.3	2.3	2.6	712	20.1	0.24
$(SiW_{12})_2$/nMCM-48	676	0.6	2.7	3.3	637	19.2	0.25
$(SiW_{12})_3$/nMCM-48	700	1.4	3.5	4.9	588	18.3	0.21
$(SiW_{12})_4$/nMCM-48	706	1.3	3.6	4.9	333	17.8	0.23

Textural properties of support as well as catalysts are shown in Table 1. Relatively small pore diameter of nMCM-48 gives the first indication that the support is nano-porous in nature with high specific surface area. Significant decrease in both, surface area as well as pore volume clearly indicate the incorporation of SiW_{12} inside the porous network of nMCM-48. It is very interesting to note down a decrease in surface area and increase in the pore value for $(SiW_{12})_4$/nMCM-48, indicating blocking of the sites because of the multilayer adsorption of TSA. Looking at the values of pore volume and pore diameter, $(SiW_{12})_3$/nMCM-48 was selected for the further study and redesignated as SiW_{12}/nMCM-48.

The N_2 adsorption-desorption isotherms of nMCM-48 and SiW_{12}/nMCM-48 (Figure 2) shows typical nature of type IV(b), conforming the formation of mesoporous structure. According to the IUPAC technical report, capillary condensation for the pores having smaller width is completely reversible with the absence of a hysteresis loop. In the present case, the obtained completely reversible isotherms are without hysteresis loop indicating the smaller width and confirming the nanoporous structure. The observation is in good agreement with the reported one[16]. The uniformity in the size of nanopores is well distinct from the sharpness of the step and position of the inflection point which is related to the diameter of pores (20.8 Å). For nMCM-48, adsorption in the mesopores is well distinct in the range of relative pressure between 0.2−0.3 which disappears for TSA/nMCM-48 indicating the effective filling of mesopores by TSA.

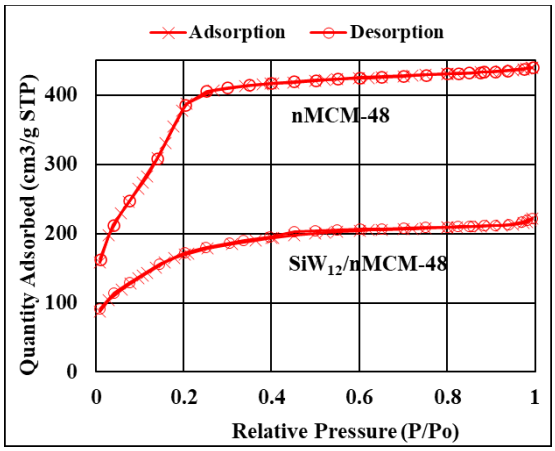

Figure 2. N_2 Adsorption-desorption isotherms of nMCM-48 and SiW_{12}/nMCM-48

The elemental analysis for SiW_{12}/nMCM-48 was carried out by EDX elemental mapping and the obtained wt % (17.34 %) of tungsten (W) was in good agreement with the theoretical calculated one (17.7 %), indicating the effective loading of SiW_{12} inside nMCM-48.

TGA for nMCM-48 and SiW_{12}/nMCM-48 are shown in figure 3. From the plots it is seen that the weight loss occurs mainly in two stages. For nMCM-48, the initial weight loss of 8.9 % up to 110 ℃ may be due to the desorption of physically absorbed water molecules. Final weight loss of <1 % up to 400 ℃ is attributed to the condensation of silanol groups present in the nMCM-48[17]. After that, no weight loss was observed, which indicates the stability up to 550 ℃. While SiW_{12}/nMCM-48, shows initial weight loss of 8.1 % up to 115 ℃ corresponding to adsorbed water. The second weight loss of 0.67 % up to 200 ℃ can be attributed to crystalline water molecules present in Keggin unit[18]. After that, no gradual weight loss up to 550 ℃, shows the stability of the catalyst.

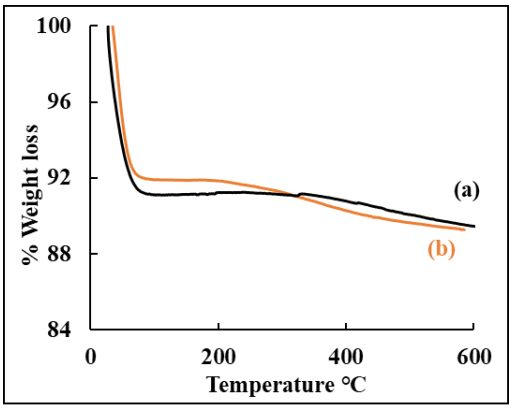

Figure 3. TGA plot of a) nMCM-48 and b) SiW_{12}/nMCM-48

In FT-IR analysis (Figure 4) the support, nMCM-48 shows characteristic bands at 462, 578 and 3448 cm-1 corresponding to the bending vibration of Si-O, symmetric stretching of Si-O-Si and the hydroxyl group of water, respectively. Observed broadband at 1100 and 1250 cm^{-1} can be attributed to the asymmetric stretching of Si-O-Si. In the case of SiW_{12}/nMCM-48, all the characteristic bands of nMCM-48 are observed along with two additional bands at 926 and 972 cm−1 which corresponds to the asymmetric vibrations of (Si-Oa) and (W-O) of keggin unit of TSA, respectively. The presence of these bands indicates the intact primary structure of the keggin unit. However, the other characteristic bands of SiW_{12} are not observed due to their superimposition with nMCM-48.

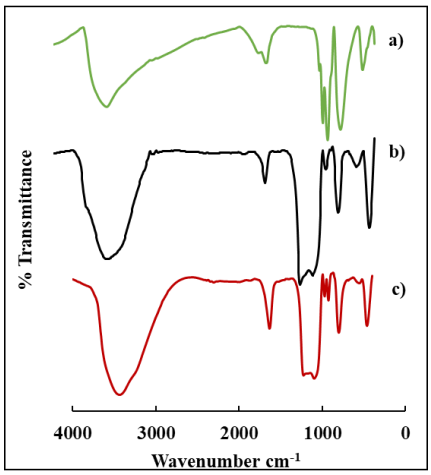

Figure 4. FT-IR spectra of a) SiW_{12} b) nMCM-48 and c) SiW_{12}/nMCM-48

The Low angle powder XRD analysis (Figure 5a) shows a typical pattern of nMCM-48 exhibiting characteristic diffraction peaks at 3.0º and 3.36º 2θ corresponding to the plane 211 and 220, respectively. In the range of 4 – 5º 2θ, numerous peaks correspond to the reflection planes 400, 321 and 420 of MCM-48 having Ia3d cubic symmetry[11]. The XRD pattern of SiW_{12}/nMCM-48 depicts the decrease in intensity of characteristic peak with slight broadening which is in good agreement with the reported one[19]. Wide angle XRD pattern (Figure 5b) of anchored MCM-48 shows the absence of characteristic peaks of the crystalline phase of SiW_{12}, signifying very fine dispersion of it into the pores of nMCM-48. Collectively, it can be inferred from the XRD results, that the structure of nMCM-48 remains intact even after impregnation of SiW_{12}.

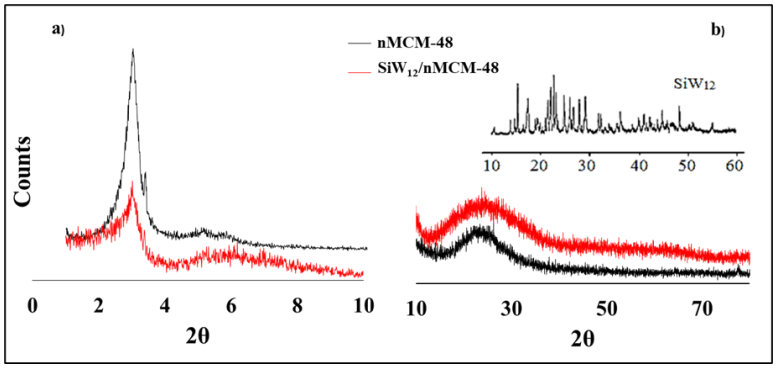

Figure 5. a) Low angle b) Wide angle Powder XRD patterns of nMCM-48 and SiW_{12}/nMCM-48

To identify the interactions between of nMCM-48 and SiW_{12}, solid state ^{29}Si MAS-NMR was performed. Typical broad peak for nMCM-48 was observed between -95 and -120 ppm corresponding to the three main components Q^2, Q^3 and Q^4 (Figure 6). The notation Q^x describes the number of x siloxane linkages to a silicon atom. For instance, the Q^2 signal corresponds to the disilanol linkage $Si\text{-}(O\text{-}Si)_2\,(\text{-}O\text{-}X)_2$, where X is H or SiW_{12}. Similarly, resonating peaks for $(O\text{-}X)\text{-}Si\text{-}(O\text{-}Si)_3$ and $Si\text{-}(O\text{-}Si)_4$ corresponds to Q^3 and Q^4 respectively. The observed values of chemical shifts for nMCM-48 are in good agreement with the reported literature [20].

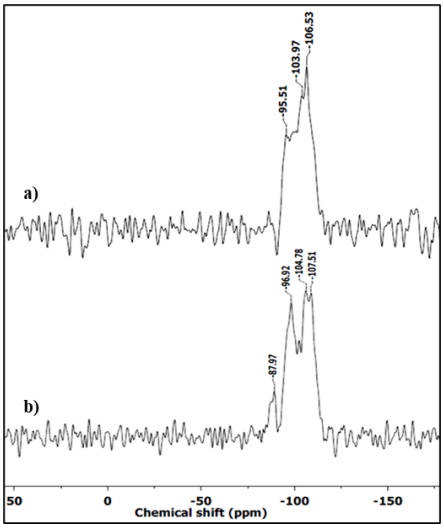

Figure 6 ^{29}Si MAS NMR spectra of a) nMCM-48 b) SiW_{12}/nMCM-48

The observed minor downfield shift in the value of chemical shift for Q^2, Q^3 and Q^4 as well as broadening in the spectrum of SiW_{12}/nMCM-48 as compared to n MCM-48 may be due to the presence of SiW_{12}. Also, a slight change in the intensities of Q^2 and Q^3 peaks were observed, indicating the strong bonding of SiW_{12} to proton of silanol groups of nMCM-48. Evidently, the

signal for SiW_{12} appears in the range of -81 to -90 ppm, which is depicted in the spectrum at -87.97 ppm, showcasing the unchanged Keggin structure of SiW_{12} [21].

SEM images (figure 7) shows spherical morphology with a uniform particle size of nMCM-48. SEM micrograph of SiW_{12}/nMCM-48 indicates the homogeneous distribution of spheres and there is no noticeable change observed in the morphology even after the introduction of SiW_{12} species, indicating its fine dispersion into three dimensional pores, further confirmed by XRD.

TEM images (Figure 8) of nMCM-48 and SiW_{12}/nMCM-48 were recorded at various magnifications. Figure 6a & 6b of nMCM-48 shows well-ordered pore networks with uniform particle diameter, confirming the nano-porous structure, which is in good agreement with the BET surface area analysis. Opaque spheres were observed in SiW_{12}/nMCM-48 (Figure 3c & 3d), where the maximum pores are uniformly filled with SiW_{12}. This is further confirmed by XRD.

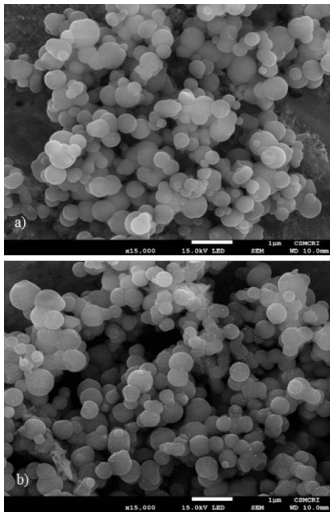

Figure 7 SEM images of a) nMCM-48 b) SiW_{12}/nMCM-48

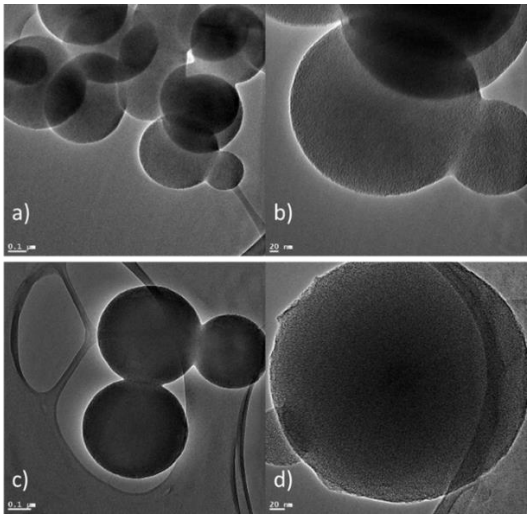

Figure 8 TEM images of a) nMCM-48 b) SiW_{12}/nMCM-48

Catalytic activity

The efficiency of SiW_{12}/nMCM-48 as a catalyst was studied for the

1. Esterification of levulinic acid with n-butanol
2. Esterification of succinic acid with n-butanol
3. Acetalization of glycerol with furfural
4. Esterification of glycerol with acetic acid

For all the transformations, detailed optimization study was performed by varying different reaction parameters, such as % loading of SiW_{12}, mole ratio of reactants, catalyst amount, temperature and time.

1. Esterification levulinic acid with n-butanol

The catalytic transformation is shown in scheme 1**.** The reaction of levulinic acid and n-butanol yields butyl levulinate, which finds ample of industrial applications, especially as a potential biofuel additive.

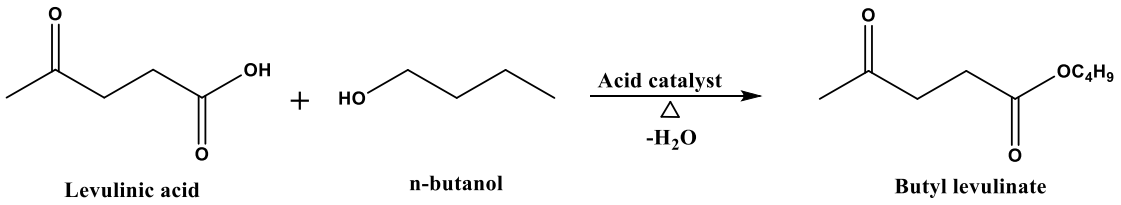

Scheme 1 Esterification levulinic acid with n-butanol

From figure 9a**,** it is seen that as the % of SiW_{12} increases, % conversion also increases from 56 to 96 %. However, the trend does not show a significant change in conversion from 30 to 40 % loading. Hence, considering the equivalent effect in terms of acidity measurements as well as % conversion, the catalyst with 30 % SiW_{12} loading, SiW_{12}/nMCM-48 was selected for the detailed study.

The effect of mole ratio of glycerol to benzaldehyde was studied by varying from 1:1 to 1:3 (Figure 9b). By increasing the ratio from 1:1 to 1:2 the % conversion of levulinic acid increases by 2% from 97 to 99%. However, on further increase the conversion decreases to 95% and hence 1:2 mole ratio was optimized.

From figure 9c, it is observed that initially, from 25 mg to 50 mg the % conversion rises from 74 to 99 %. Increase in the catalyst amount to 75 mg did not show any significant effect in terms of conversion. The observed behavior is may be due to the blocking of sites/ saturation of the number of active sites available vs. reactant amount. Hence, 50 mg was considered to be optimum amount.

The most important parameter which governs the equilibrium of reaction is the reaction temperature. As depicted by the plot in figure 9d, with temperature, the reaction proceeds significantly giving 99% at 90 ℃. After that there was no major rise in the % conversion. Therefore, an easily accessible temperature, 90 ℃ was optimized.

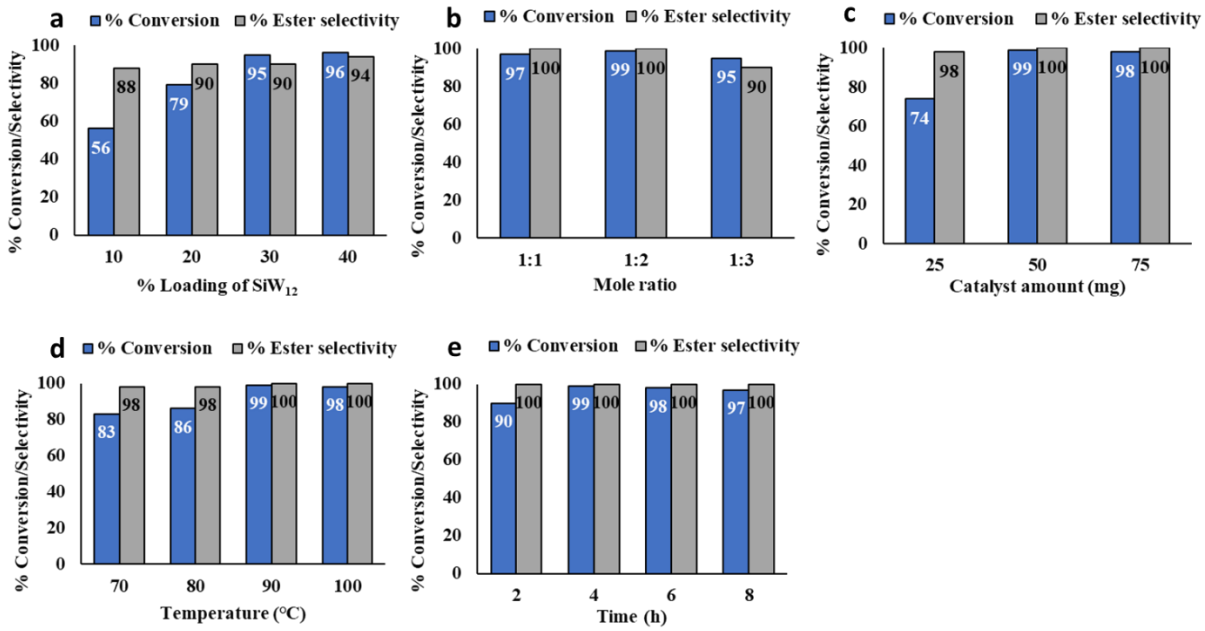

Figure 9. Reaction conditions: a) Effect of % loading of SiW_{12}. Mole ratio 1:2; Catalyst amount 50 mg; Temperature 90℃; Time 4h, b) Effect of mole ratio. Catalyst amount 50 mg; Temperature 90℃; Time 4h, c) Effect of catalyst amount. Mole ratio 1:2; Temperature 90℃; Time 4h, d) Effect of temperature. Mole ratio 1:2; Catalyst amount 50 mg; Time 4h, e) Effect of time. Mole ratio 1:2; Catalyst amount 50 mg; Temperature 90℃.

From figure 9e it is seen that % conversion increased from 2 to 4h, with no change in the selectivity of ester. Despite increasing the reaction time up to 8 h, a negligible decrement of 2 % in conversion was observed which indicates the establishment of equilibrium. Thus, 4h was considered to be optimum time for reaction.

The optimized reaction conditions for the maximum conversion of levulinic acid (99 %) and selectivity of ester (100 %) are, mole ratio (levulinic acid: n-butanol) 1: 2; catalyst amount 50 mg; temperature 90 ℃; time 4h with TON 2469 and TOF of 617 h^{-1}.

2. Esterification Succinic acid with n-butanol

Esterification reaction between succinic acid and n-butanol yields two ester products- monobutyl succinate (monoester) and dibutyl succinate (diester) (scheme 2) and the results obtained from the optimization study are shown in figure 10.

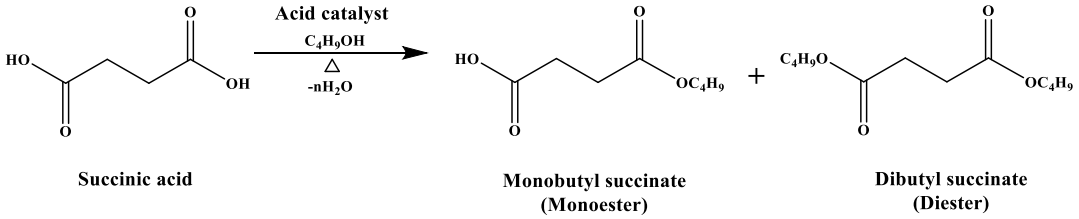

Scheme 2 Esterification of succinic acid with n-butanol

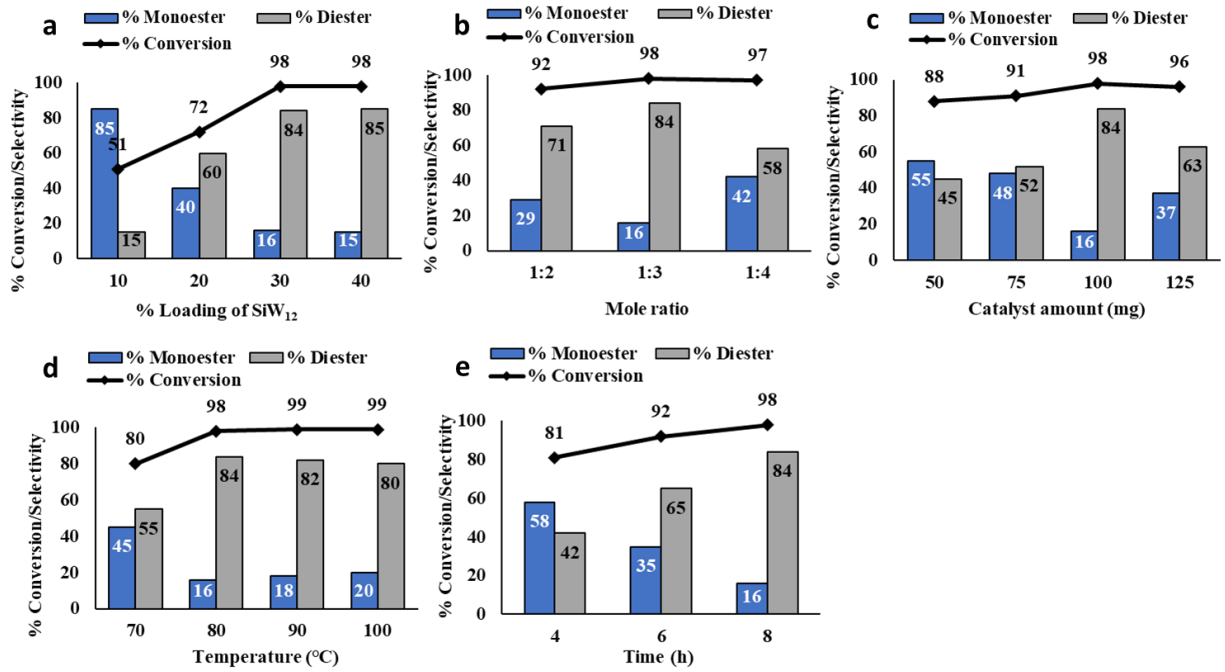

Figure 10. Reaction conditions: a) Effect of % loading of SiW_{12}. Mole ratio 1:3; Catalyst amount 100 mg; Temperature 80℃; Time 8h, b) Effect of mole ratio. Catalyst amount 100 mg; Temperature 80℃; Time 8h, c) Effect of catalyst amount. Mole ratio 1:3; Temperature 80℃; Time 8h, d) Effect of temperature. Mole ratio 1:3; Catalyst amount 100 mg; Time 8h, e) Effect of time. Mole ratio 1:3; Catalyst amount 100 mg; Temperature 80℃.

The optimum conditions for the catalytic reaction are, mole ratio (Succinic acid: n-butanol)- 1:3; catalyst amount- 100 mg; temperature- 80 ℃ and time- 8h. The maximum conversion of 98%

and selectivity of diester (84%) was achieved in the above optimized conditions with the TON 1227 and TOF of 153 h^{-1}.

3. Acetalization of glycerol with furfural

The acetalization of glycerol with furfural yields two cyclic products, 1,3-dioxolane (5-membered) and 1,3 dioxane (6- membered), shown in scheme 3 and the results obtained from the optimization study are shown in figure 11.

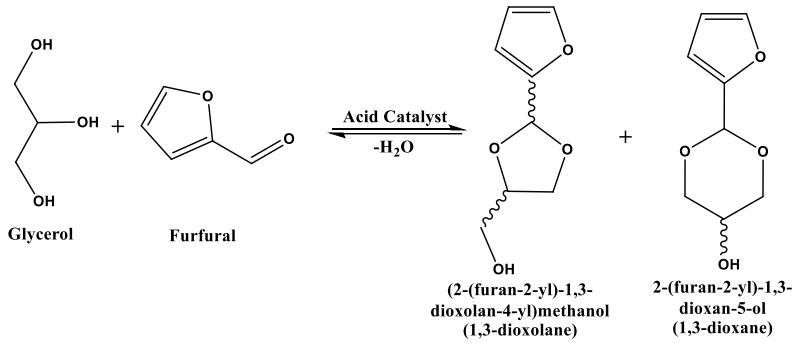

Scheme 3 Acetalization of glycerol with furfural

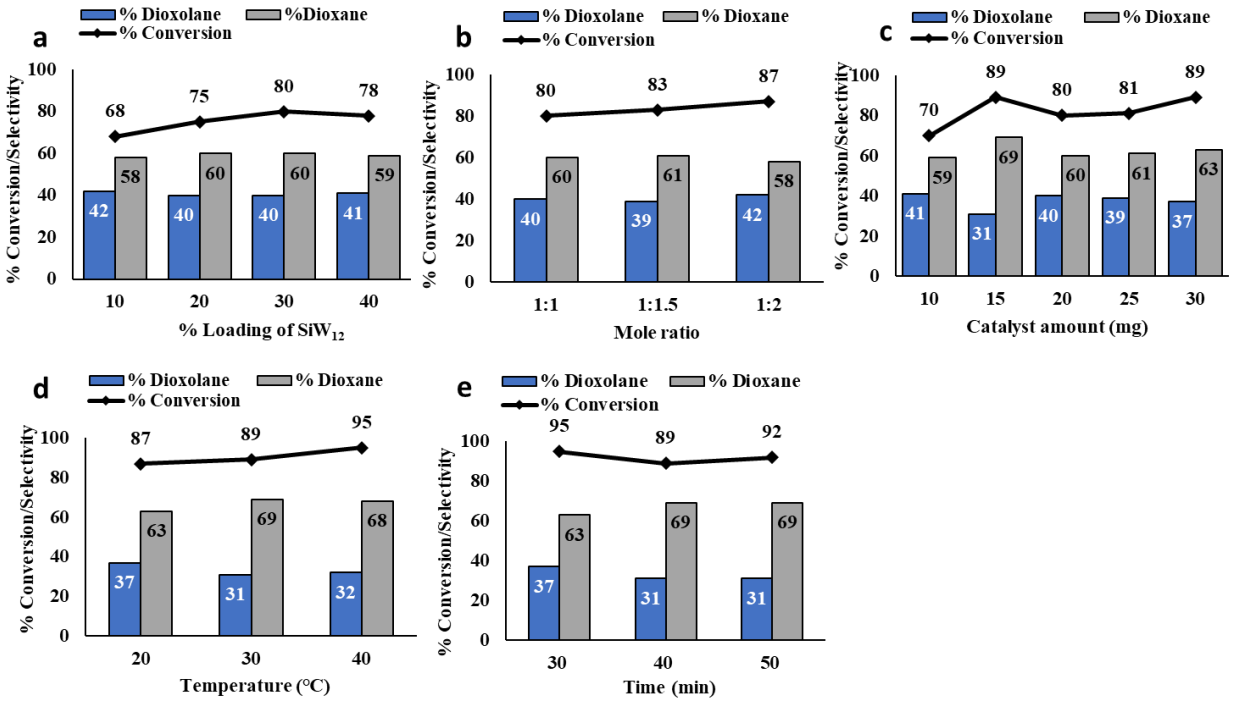

Figure 11. Reaction conditions: a) Effect of % Loading of SiW_{12}. Mole ratio 1:1; Catalyst amount 20 mg; Temperature 30°C; Time 40 min, b) Effect of mole ratio. Catalyst amount 20 mg; Temperature 30°C; Time 40 min, c) Effect of catalyst amount. Mole ratio 1:1; Temperature 30°C; Time 40 min, d) Effect of temperature. Mole ratio 1:1; Catalyst amount 15 mg; Time 40 min, e) Effect of time. Mole ratio 1:1; Catalyst amount 15 mg; Temperature 30°C.

The optimum conditions for glycerol acetalization with furfural for maximum conversion (89 %) and selectivity (69 %) towards dioxane are: Mole ratio (glycerol: furfural) 1:1; catalyst amount 15 mg; temperature 30 ℃; time 40 min with TON 7355 and TOF of 10978 h^{-1}.

4. Esterification of glycerol with acetic acid

The esterification reaction of glycerol was carried out with acetic acid and the obtained products; monoacetyl glycerol (MAG), diacetyl glycerol (DAG) and triacetyl glycerol (TAG) are shown in scheme 4. The results obtained from the optimization study are shown in figure 12.

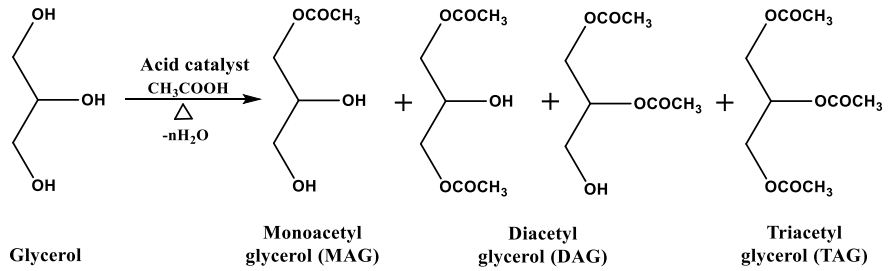

Scheme 4 Esterification of glycerol with acetic acid

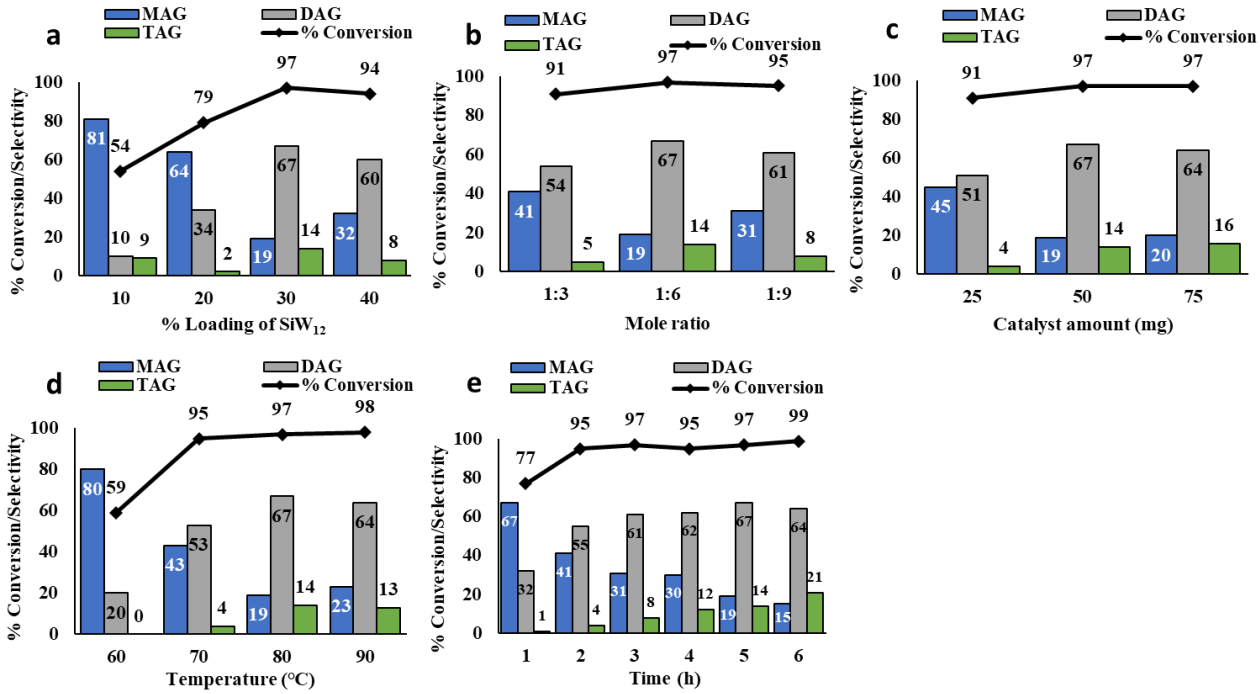

Figure 12. Reaction conditions: a) Effect of % Loading of SiW_{12}. Mole ratio 1:6; Catalyst amount 50 mg; Temperature 80°C; Time 5 h, b) Effect of mole ratio. Catalyst amount 50 mg; Temperature 80°C; Time 5 h, c) Effect of catalyst amount. Mole ratio 1:6; Temperature 80°C; Time 5 h, d) Effect of temperature. Mole ratio 1:6; Catalyst amount 50 mg; Time 5 h, e) Effect of time. Mole ratio 1:6; Catalyst amount 50 mg; Temperature 80°C.

The optimized reaction parameters for esterification glycerol with acetic acid are: mole ratio (glycerol: acetic acid)- 1:6; catalyst amount- 50 mg; reaction temperature- 80 ℃; reaction time- 5h. These conditions lead to 97% of glycerol with the selectivity of 19%, 67% and 14% towards MAG, DAG and TAG respectively with a TON of 2420 and TOF of 484 h^{-1}.

Kinetic experiments were also carried out to determine the activation energy by using the Arrhenius equation and the probable mechanistic pathway was proposed for all the reactions.

The control experiments with alone support nMCM-48 as well as SiW_{12} were performed in the respective optimized conditions for all the reactions. It was observed that alone nMCM-48 was not very active, indicating that the SiW_{12} is the active species responsible for the catalytic activity. Thus, retention of activity of SiW_{12} in the catalyst suggests that we were successful in developing of a truly heterogeneous catalyst. Furthermore, the recycling experiments were carried out for all the transformations and the catalyst showed its stability for multiple runs. The recycled catalyst was also characterized for acidity measurements, BET surface area analysis and FT-IR, indicating its unaltered nature after the catalytic cycles.

Chapter 2: Mono lacunary Silicotungstate (SiW_{11}) anchored to MCM-48: Synthesis, characterization and esterification as well as acetalization reactions

Synthesis of mono lacunary silicotungstate (SiW_{11})

The mono lacunary silicotungstate was synthesized by following the method reported by Brevard et al. [10]. 0.22 mol, 7.2 g sodium tungstate and 0.02 mol,0.56 g sodium silicate was dissolved in 150 mL distilled water at 80° C. The pH was adjusted to 4.8 by dilute nitric acid. The volume of the mixture was reduced to half and the resulting solution was filtered to remove un-reacted silicates. The lacunary polyoxometalate anion was separated by liquid-liquid extraction with acetone. The extracted sodium salt of mono lacunary silicotungstate was dried at room temperature in air and the resulting material was designated as SiW_{11}.

Synthesis of series of catalysts, containing 10 - 40 % of SiW_{11} was carried out by the similar impregnation method as mentioned previously (chapter 1) followed by treatment with 0.1 N HCl solution and preliminary characterizations were done by acidity measurements (potentiometric titration), BET surface area and pore size distribution, TGA, FT-IR, XRD, ^{29}Si MAS-NMR, and

TEM. Further characterization for the catalyst is in progress. Here also, from acidity measurements and surface area

Similar to previous chapter, the catalytic activity for SiW_{11}/nMCM-48 was carried out for levulinic acid and succinic acid esterification with n-butanol along with detailed optimization study.

The optimized conditions for esterification of levulinic acid with n-butanol for maximum conversion (49%) as well as selectivity (84% ester) are, mole ratio 1:2; catalyst amount 50 mg; temperature 90 ℃; time 4h, with TON of 1300 and TOF of 325 h^{-1}.

The optimized conditions for esterification of succinic acid with n-butanol for maximum conversion (83%) as well as selectivity (43% diester) are, mole ratio 1:3; catalyst amount 75 mg; temperature 90 ℃; time 8h, with TON of 1466 and TOF of 183 h^{-1}.

The activation energy for both the reactions were determined and the control experiments suggests the true heterogeneous nature of catalyst. Furthermore, the recycling studies were performed and suggests its reusability up to multiple runs. The characterization of regenerated catalyst was also carried out similar to previous chapter.

Preliminary catalytic studies for the acetalization of glycerol with furfural and esterification of glycerol with acetic acid was carried out. The detailed optimization study for both the reactions are in progress.

Part B

Chapter 1: Parent Silicotungstic acid (SiW_{12}) anchored to MCM-22: Synthesis, characterization and esterification as well as acetalization reactions

The zeolitic support MCM-22 was acquired commercially and a series of catalysts comprising 10 – 40 % of SiW_{12} anchored to MCM-22 was prepared by the method mentioned in Part A chapter 1. A detailed characterization of the support and synthesized catalyst, using different physicochemical techniques (Acidity measurements (Potentiometric titration), BET surface area analysis and pore size distribution, elemental analysis, TGA, FT-IR, Powder XRD, ^{29}Si MAS NMR, SEM and TEM) was carried.

FT-IR spectra of SiW_{12}, MCM-22 and SiW_{12}/MCM-22 are shown in figure 13. FT-IR of MCM-22 shows characteristic bands at 3441 cm^{-1}, 1635 cm^{-1}, 1226 cm^{-1}, 817 cm^{-1} and 455 cm^{-1}. Band at 3441 is due to the to the O-H stretching of hydroxyl group of loosely bound water molecules. At 817 cm^{-1} and 1226 cm^{-1}, the bands are attributed to the symmetric and asymmetric stretching of T-O-T bond respectively, where T= Si or Al. Stretching vibration corresponding to T-O, where the metal ion is bonded to four oxygen atoms is observed at 455 cm^{-1}. FT-IR of SiW_{12}/MCM-22 shows an additional band at 925 cm^{-1}, one of the characteristic bands for Keggin unit of SiW_{12} corresponding to asymmetric vibration of (Si-Oa). However, the other bands are not distinct due to their superimposition with that of support. Presence of this fingerprint band suggests that the primary of Keggin unit is intact even after impregnation on the support.

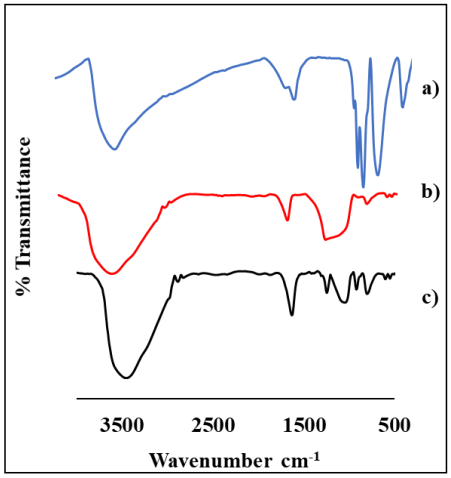

Figure 13 FT-IR spectra of a) SiW_{12} b) MCM-22 and c) SiW_{12}/MCM-22

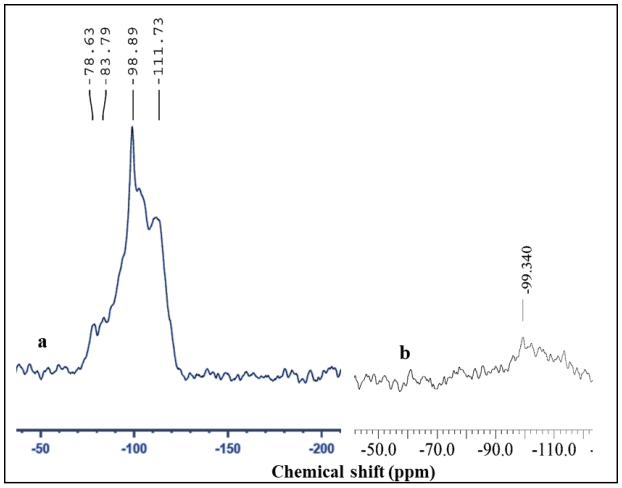

Figure 14 ^{29}Si MAS NMR of a) SiW_{12}/MCM-22 b) MCM-22

The ^{29}Si MAS NMR for MCM-22 (Figure 14) shows distinct peak at -99.34 ppm corresponding to the Si associated with one Al unit and a range of small peaks from –102 to -118 ppm due to the other Si (which are not surrounded by Al atoms) present in MCM-22. In the NMR spectra of SiW_{12}/MCM-22 (Figure 14), the first peak shifts slightly to -98 ppm. It is interesting to note, the intensities of the bunch of peaks (-100.84 to -113.6 ppm) rises, indicating an increase of Si in the framework. These extra sites come from SiW_{12}, suggesting the firm interaction of it with the support framework.

SEM images of MCM-22 and SiW_{12}/MCM-22 are shown in figure 15. From the images, morphology of MCM-22 appears to have very thin platelets which are interpenetrating each other and forms a lamellar particle. It is noteworthy that even after impregnation of SiW_{12}, there is no alteration as well as aggregation observed in the lamellar structure of MCM-22, indicating the stable morphology of the catalyst.

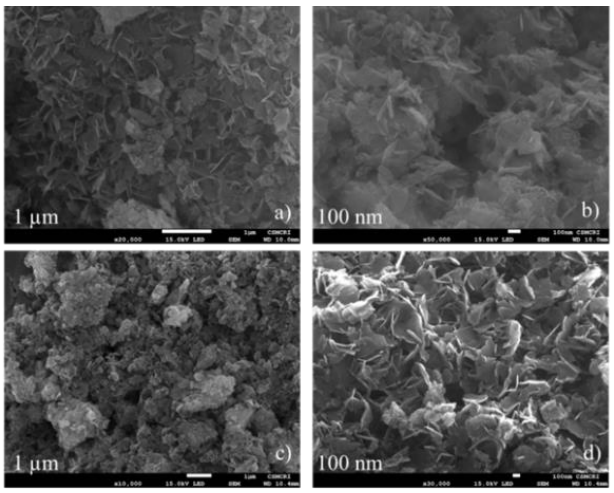

Figure 15. SEM images of a), b) MCM-22 and c), d) SiW_{12}/MCM-22

Detailed optimization study for esterification of levulinic acid with n-butanol, esterification of succinic acid with n-butanol as well as acetalization of glycerol with furfural was carried out by varying different reaction parameters.

The optimized conditions for esterification of levulinic acid with n-butanol for maximum conversion (65%) as well as selectivity (94% ester) are, mole ratio 1:2; catalyst amount 50 mg; temperature 90 ℃; time 8h, with TON of 1621 and TOF of 203 h^{-1}.

The optimized conditions for esterification of succinic acid acid with n-butanol for maximum conversion (97%) as well as selectivity (59% ester) are, mole ratio 1:3; catalyst amount 100 mg; temperature 90 ℃; time 10h, with TON of 1214 and TOF of 121 h^{-1}.

The optimized conditions for acetalization of glycerol with furfural for maximum conversion (63%) as well as selectivity (66% dioxane) are, mole ratio 1:2; catalyst amount 30 mg; temperature 30 ℃; time 40 min, with TON of 2625 and TOF of 3918 h^{-1}.

For all the reactions, activation energy was calculated and determined by using Arrhenius equation. The control experiments indicate the synergistic effect of SiW_{12} and MCM-22 thus forming a truly heterogeneous catalyst. The recycling experiments were performed and suggests its sustainable nature and reusability up to multiple runs. The characterization of regenerated catalyst was also carried out similar to previous chapter and a probable mechanistic pathway for all the reactions was proposed.

Preliminary catalytic studies for the esterification of glycerol with acetic acid was carried out and the detailed optimization study is in progress.

Chapter 2: Mono lacunary silicotungstate (SiW_{11}) anchored to MCM-22: Synthesis, characterization and esterification as well as acetalization reactions

A series of catalysts with 10 – 40 % of SiW_{11} anchored to MCM-22 was prepared by the method mentioned in Part A chapter 1 followed by treatment with 0.1 N HCl solution. Preliminary Characterization of the synthesized catalyst was carried out by different physicochemical techniques and here also from acidity measurements as well as BET surface area analysis, 30 % loading of SiW_{11} (SiW_{11}/MCM-22) on MCM-22 was found to be optimum amount. Further characterization of the catalyst is under progress.

The catalytic activity was evaluated for the esterification of levulinic acid with n-butanol and a detailed optimization study was carried out by varying different reaction parameters.

The optimized conditions for esterification of levulinic acid with n-butanol for maximum conversion (78%) as well as selectivity (94% ester) are, mole ratio 1:2; catalyst amount 50 mg; temperature 90 ℃; time 14h, with TON of 2069 and TOF of 148 h^{-1}.

The activation energy for levulinic acid esterification was calculated and determined by using Arrhenius equation. The control experiments with alone SiW_{11} and MCM-22 was carried out, indicating the successful formation of a truly heterogeneous catalyst. The recycling experiments were performed indicated its reusability up to multiple runs. The characterization of regenerated catalyst was also carried out.

Preliminary catalytic studies for the esterification of succinic acid with n-butanol, acetalization of glycerol with acetic acid as well as glycerol with acetic acid was carried out and the detailed optimization study for all the reactions is in progress.

Comparison of activity of the synthesized catalysts

The catalytic activity of all four synthesized catalyst was compared for levulinic acid esterification by keeping the reaction in similar conditions and the obtained results are shown in table 2.

Table 2 Levulinic acid esterification with all catalysts

Reaction	Catalyst	Surface area (m^2/g)	Acidic strength, mV	% Conv/Sel	TON/TOF, h^{-1}
Esterification of Levulinic acid	SiW_{12}/nMCM-48	588	700	99/100	2469/617
	SiW_{11}/nMCM-48	516	460	49/84	1300/325
	SiW_{12}/MCM-22	234	456	38/94	948/240
	SiW_{11}/MCM-22	324	390	32/78	849/212

It is observed that SiW_{12}/nMCM-48 exhibits excellent catalytic activity for the esterification of levulinic acid as compared to that of SiW_{11}/nMCM-48. Similarly, SiW_{12}/MCM-22 shows better results relative to SiW_{11}/MCM-22. This observed difference may be correlated to the nature of active species as well as the acidity of the catalysts. Thus, **SiW_{12}/nMCM-48** and **SiW_{12}/MCM-22**, were selected as the **two good catalysts** from the synthesized ones. Also, in both catalysts, the active species SiW_{12} was found to be common which indicates that the acidity of active species plays an important role in governing the esterification reaction.

Furthermore, the activity of both the supports nMCM-48 and MCM-22 was compared keeping the active species (SiW_{12}/SiW_{11}) constant. It is observed that the catalysts with nMCM-48 as support showed admirable catalytic activity as compared to that of MCM-22 based catalyst. This

observed difference in the catalytic activity can be correlated to their unique structures and pore networks. MCM-22 possesses 2D sinusoidal channels with layered structure and is zeolitic in nature having Al sites as Lewis acid sites while nMCM-48 is purely silicious, exhibits 3D branched channels with cubic mesophase. It also possesses higher surface area. These properties benefit the strong hold of active species and increases their surface area tremendously. The 3D cubic structure as well as the higher surface area of nMCM-48 based catalysts, provides a larger access of reactants to acidic sites and also promotes the outgoing products. Hence, for the catalytic activity **nMCM-48** comes out to be the **better support** as compared to that of MCM-22.

Henceforth, looking to the highest acidity, 3D cubic structure and highest surface area, **SiW_{12}/nMCM-48** was found to be the **best catalyst** amongst the synthesized ones.

Annexure

Catalytic degradation of some organic dyes over SiW_{12} anchored nMCM-48 and MCM-22 catalysts

Dyes are primarily used in paints, textiles, printing inks, paper, and plastics that are majorly associated with textile industry. The natural dyes were replaced by chemical dyes that can bind to the fabric for longer time and retain colour throughout washing and exposure. The chemical dyes are generally soluble and organic in nature and hence it is difficult to remove them by conventional methods. Exposure to dye-bearing waste water exhibits severe harmful effect causing an environmental pollution, and it is also associated with health hazards as the degradation products of dyes are carcinogenic in nature. Due to the adverse treatment of dye water is mandatory before submerging it with natural water bodies.

In this regard, the versatility of the selected two good catalysts, **SiW_{12}/nMCM-48** and **SiW_{12}/MCM-22,** the catalytic activity was investigated for the degradation of some cationic dyes like methylene blue (MB), crystal violet (CV), and an azo dye chrysoidine Y (CY).

Various reaction parameters like dye concentration, catalyst amount, and reaction time were investigated and the degradation efficiency with SiW_{12}/MCM-22, was found to be 95% for MB,

90% for CV and 84% for CY in the optimised reaction (100 ppm dye concentration, 2.5 mg/ml catalyst and reaction time 60 min.

The catalytic degradation of MB was studied using SiW_{12}/nMCM-48 and degradation efficiency was found to be 98% under the conditions: dye concentration, 100 ppm; catalyst dosage, 10 mg; time, 60 mins. The degradation studies with CV and CY are under progress.

Excellent results with both the catalysts validate their multipurpose catalytic activity.

Summary

The acidic property of parent silicotungstic acid (SiW_{12}) has been tuned by formation of mono lacunary silicotungstate (SiW_{11}) and the nanoporous support, nMCM-48 was successfully synthesized. Environmentally benign, green and sustainable heterogeneous catalysts based on SiW_{12} /SiW_{11} and nMCM-48/MCM-22 (SiW_{12}/nMCM-48, SiW_{11}/nMCM-48, SiW_{12}/MCM-22 and SiW_{11}/MCM-22) were successfully synthesized and characterized using acidity measurements (Potentiometric titration), BET surface area analysis and pore size distribution, elemental analysis, TGA, FT-IR, Powder XRD, ^{29}Si MAS NMR, SEM and TEM. Some of the characterization of SiW_{11}/nMCM-48 and SiW_{11}/MCM-22 are in progress.

Versatile catalytic applications of the synthesized catalysts were established via esterification and acetalization reactions of important bioplatform molecules and the catalysts were able to selectively catalyze the process for the synthesis of biofuel additives. The detailed optimization studies for all the transformations with SiW_{12}/nMCM-48 was successfully carried out while the same with SiW_{11}/nMCM-48, SiW_{12}/MCM-22 and SiW_{11}/MCM-22 for some transformations is in progress.

For levulinic acid esterification, the activities of SiW_{12} based catalysts were higher than SiW_{11} and nMCM-48 comes out to be a better support amongst the two supports, thus giving SiW_{12}/nMCM-48 as the best catalyst among the synthesized ones.

Also, the synthesized catalyst showed outstanding activity for the catalytic degradation of organic dyes, which corroborates its flexible nature for other transformations as well.

References

1 J. C. Serrano-Ruiz, R. Luque and A. Sepúlveda-Escribano, *Chemical Society Reviews*, 2011, **40**, 5266–5281.

2 A. M. Raspolli Galletti, C. Antonetti, S. Fulignati and D. Licursi, *Catalysts*, 2020, **10**, 1–2.

3 C. Antonetti, D. Licursi, S. Fulignati, G. Valentini and A. M. R. Galletti, *Catalysts*, 2016, **6**, 1–29.

4 M. Hara, K. Nakajima and K. Kamata, *Science and Technology of Advanced Materials*, 2015, **16**, 34903.

5 B. Saikia and D. Gandhi, *Internation Journal Of Advance Research And Innovative Ideas In Education*, 2017, 3, 70–95.

6 I. v Kozhevnikov, *Chemical Reviews*, 1998, **98**, 171–198.

7 M. Misono, I. Ono, G. Koyano and A. Aoshima, *Pure and Applied Chemistry*, 2000, **72**, 1305–1311.

8 T. Okuhara, N. Mizuno and M. Misono, eds. D. D. Eley, W. O. Haag and B. B. T.-A. in C. Gates, Academic Press, 1996, vol. 41, pp. 113–252.

9 N. Mizuno, S. Hikichi, K. Yamaguchi, S. Uchida, Y. Nakagawa, K. Uehara and K. Kamata, *Catalysis Today*, 2006, **117**, 32–36.

10 N. Mizuno, K. Yamaguchi and K. Kamata, *Coordination Chemistry Reviews*, 2005, **249**, 1944–1956.

11 J. Xu, Z. Luan, H. He, W. Zhou and L. Kevan, *Chemistry of Materials*, 1998, **10**, 3690–3698.

12 D. Kumar, K. Schumacher, C. du Fresne von Hohenesche, M. Grün and K. K. Unger, *Colloids and Surfaces A: Physicochemical and Engineering Aspects*, 2001, **187–188**, 109–116.

13 V. A. Ostroumova and A. L. Maksimov, *Petroleum Chemistry*, 2019, **59**, 788–801.

14 C. Delitala, M. D. Alba, A. I. Becerro, D. Delpiano, D. Meloni, E. Musu and I. Ferino, *Microporous and Mesoporous Materials*, 2009, **118**, 1–10.

15 P. Ferreira, I. M. Fonseca, A. M. Ramos, J. Vital and J. E. Castanheiro, *Applied Catalysis B: Environmental*, 2010, **98**, 94–99.

16 M. Thommes, K. Kaneko, A. v Neimark, J. P. Olivier, F. Rodriguez-Reinoso, J. Rouquerol and K. S. W. Sing, *Pure and Applied Chemistry*, 2015, **87**, 1051–1069.

17 S. Singh and A. Patel, *Journal of Cleaner Production*, 2014, **72**, 46–56.

18 N. Narkhede and A. Patel, *Applied Catalysis A: General*, 2016, **515**, 154–163.

19 A. Sakthivel, K. Komura and Y. Sugi, *Industrial and Engineering Chemistry Research*, 2008, **47**, 2538–2544.

20 V. Dellarocca, L. Marchese, M. L. Peña, F. Rey, A. Corma and S. Coluccia, *Studies in Surface Science and Catalysis*, 2001, **140**, 209–220.

21 F. J. Berry, G. R. Derrick and M. Mortimer, *Polyhedron*, 2014, **68**, 17–22.

Dhruvi Pithadia
Research Scholar

Prof. (Dr.) Anjali Patel
Research Supervisor

Prof. Dr. Anjali Patel
Chemistry Dept., Faculty of Science
The M. S. University of Baroda
Vadodara.

Prof. Ashutosh Bedekar
Offg. Head
Department of Chemistry

HEAD
Department of Chemistry
Faculty of Science
The Maharaja Sayajirao University of Baroda
Vadodara - 390002. Gujarat - INDIA